Electronic Supplementary Material (ESI) for Chemical science
This jiounal is © the Royal Society of Chemistry 2011

Supporting Information for

A Unique Substituted Co(II)–Formate Coordination Framework Exhibits Weak Ferromagnetic Single-Chain-Magnet Like Behavior

Jiong-Peng Zhao,[a,b] Qian Yang,[a] Zhong-Yi Liu,[c] Ran Zhao,[a] Bo-Wen Hu,[a] Miao Du,[c] Ze Chang,[a] and Xian-He Bu[a]*

* Corresponding author. Fax: (+86) 22-23502458. E-mail: buxh@nankai.edu.cn

Table S1. *Selected bond lengths [Å] and angles [°] for* ***1****.*

Co1—O6	1.968 (4)	Co2—O2	2.053 (5)
Co1—O1	2.094 (5)	Co2—O7^{ii}	2.086 (5)
Co1—O3	2.094 (5)	Co2—O7^{iii}	2.094 (5)
Co1—O4	2.162 (5)	Co2—O7	2.126 (5)
Co1—N1^{i}	2.178 (6)	Co2—O4	2.153 (5)
Co1—O5	2.271 (5)	Co2—O5	2.154 (5)
Co1^{iv}—O6—Co1	118.4 (3)	Co2—O7—Co2^{iii}	90.56 (19)
Co2—O4—Co1	101.9 (2)	Co2^{ii}—O7—Co2^{iii}	102.9 (2)
Co2—O5—Co1	98.4 (2)	Co2^{ii}—O7—Co2	96.1 (2)

Symmetry Code: ^{i} *y−1, −x+1, −z+3/2;* ^{ii} *−y+3/2, −x+3/2, −z+3/2;* ^{iii} *y−1/2, x+1/2, −z+3/2;* ^{iv} *x, y, −z+2*

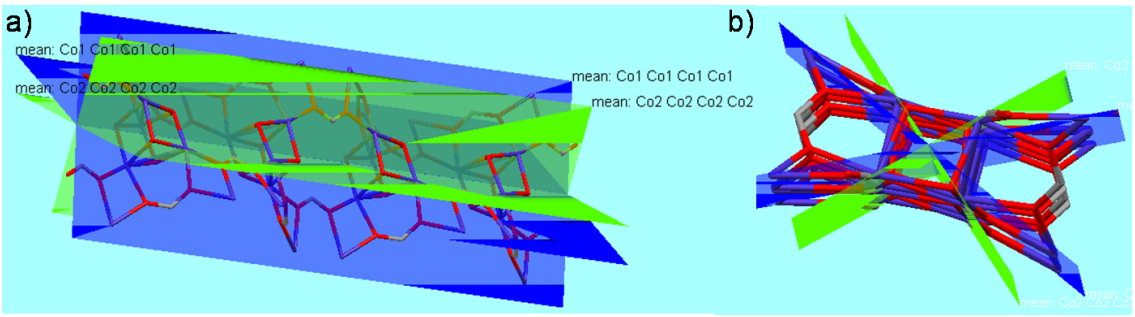

Fig. S1 a) Side and b) perspective views of four different planes defined by Co1 and Co2 ions in the 1D chain. The dihedral angle between Co1-plane and Co2-plane in the neighbor rings is 67.51°, and the dihedral angle between the same-atom planes in the neighbor rings is 49.43° for Co1 and 85.60° for Co2.

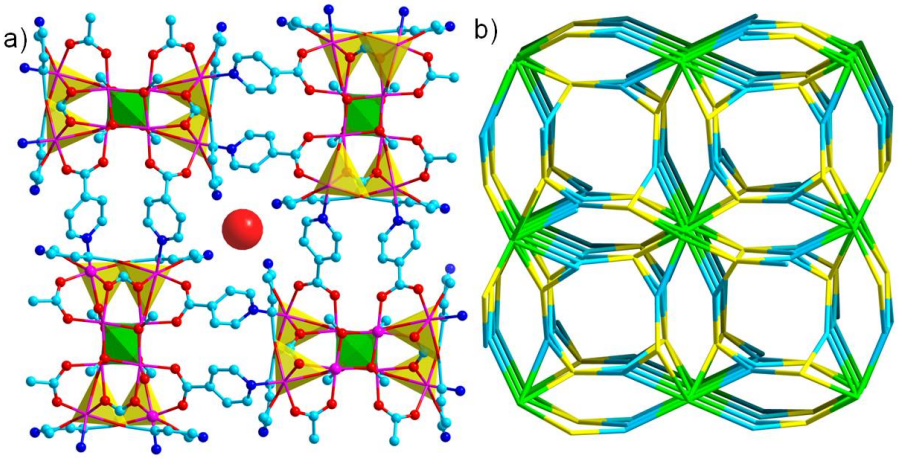

Fig. S2 (a) The 3D framework of **1** (C in cyan, O in red, N in blue, Co in pink). (b) The (3,6,8)-connected topological network of **1**. The cyan, yellow, and green spheres represent the 3-, 6-, and 8-connected nodes, respectively.

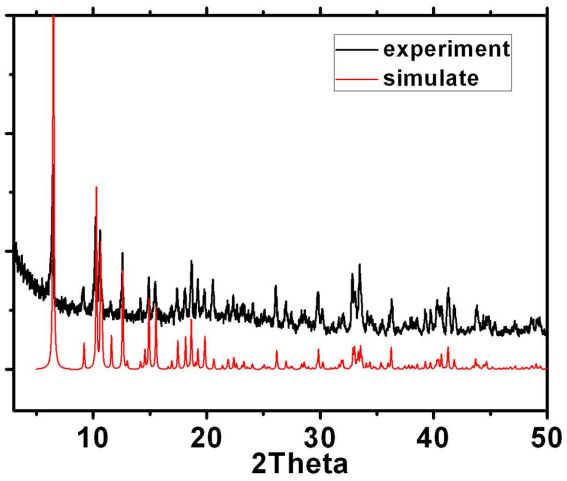

Fig. S3 X-ray powder diffraction (XRPD) patterns of **1**.

Magnetic measurements

The magnetic measurements were performed by using an MPMS XL-5 SQUID magnetometer with polycrystals of **1**. With the help of a ^{3}He system （at Tianjin Normal University）, measurements can be performed down to 0.5 K. Diamagnetic corrections were estimated by using Pascal constants and background corrections by experimental measurement on sample holders.

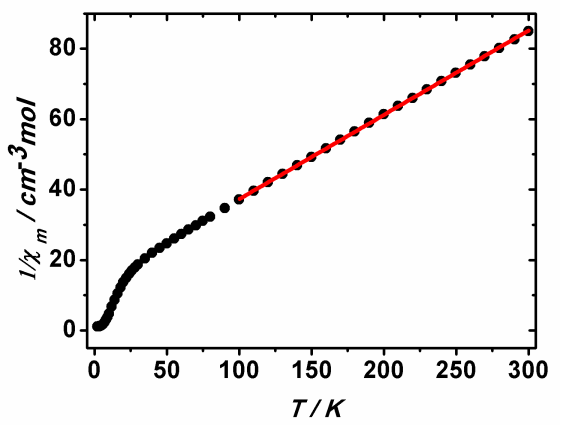

Fig. S4 The Curie-Weiss plot of **1**. Solid line represents the best fit.

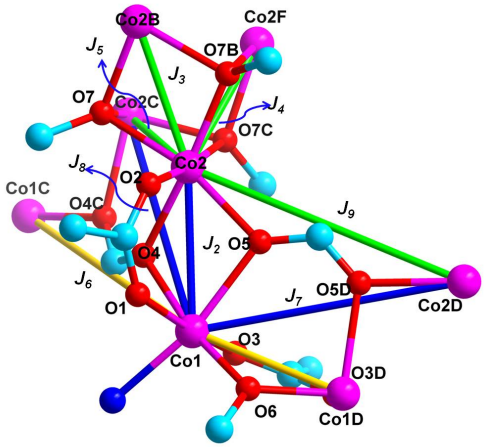

Fig. S5 Magnetic exchange ways between the Co^{II} ions in **1**.

Table S2 The number and type of the exchange ways between the Co^{II} ions and the nature interactions in the chain of **1** as well as some weak ferromagnetism system with simila briding mode.

coupling	metal ions	Number of bridges				M-O-M(°)	M-M distances(Å)	interactions	Ref:
		syn-syn	syn-anti	anti-anti	μ-O				
J_1	Co1-Co1D	2			1	118.4 (3)	3.378	AF	1 ,2
J_2	Co1-Co2	1			2	101.9 (2) /98.4 (2)	3.352	AF	3
J_3	Co2-Co2B				2	96.1 (2)	3.132	AF	4a
J_4	Co2-Co2F				2	102.9 (2)	3.269	AF	4a
J_5	Co2-Co2C	1			2	90.56 (19)	2.998	AF	3
J_6	Co1-Co1C			1			6.146	Weak AF or F	5a,c
J_7	Co1-Co2D		1				5.669	Weak AF or F	5a,c
J_8	Co1-Co2C		1				5.423	Weak AF or F	5a,c
J_9	Co2-Co2D			1			6.189	Weak AF or F	5a,c

Co1 and Co2 ions are all in a slightly compressed octahedral geometry with O1, O3 and O2, O7 in the apical positions. And the axis of the neighbouring Co^{II} octahedrons tilt to each other in the ring and parallel Co^{II} octahedrons could be found in in interval rings (Fig 2a). The bridges could be classified as four different type, μ-O atom, *syn,syn, syn.anti* and *anti,anti* carboxylate (including formate) (Fig S4 and Table S2). The interactions conducted by the *μ-O atom* dependent on the Co-O-Co angle. Large Co-O-Co angles lead to antiferromagnetic interactions while small ones

induce ferromagnetic coupling with critical angle about 90°. The *syn,syn* carboxylate conduct stronger antiferromagnetic interactions between metal ions, while others conduct weak ferro-or antiferromagnetic interactions. Thus, the coupling J_1, J_2, J_3, J_4 and J_5 are antiferromagnetic,[1,2,3,4,5] while the interactions of J_6, J_6, J_8, and J_9 should be weak ferro- or antiferromagnetic.[6] Taking spin-canting into account two factors need to be considered: the antisymmetric interaction (Dzyaloshinsky-Moriya interaction, DMI) and the magnetic anisotropy.[6] The ions in the Co1 dimer and the Co2 tetrahedron are all asymmetric and the neighbouring Co^{II} octahedrons tilt to each other. Furthermore the Co^{II} ions show significant anisotropy, thus spin canting may occur in the asymmetric arranged Co^{II} chain. Also, the spin competition resulted from antiferromagnetic interactions between the Co2 tetrahedrons may contribute to the spin canting. The interactions conducted by the *syn,syn* carboxylate and μ-O atom are dominate, and the mainly canted antiferromagnetic interactions in the chains could be predigested in Fig 2b (blue line).

References:

1 K. C. Mondal, G. E. Kostakis, Y. Lan, C. E. Anson, A. K. Powell, *Inorg. Chem. 2009*, **48**, 9205.
2 Z.-M. Wang, B. Zhang, M. Kurmoo, M. A. Green, H. Fujiwara, T. Otsuka, H. Kobayashi, *Inorg. Chem. 2005*, **44**, 1230.
3 S. M. Humphrey, Paul T. Wood, *J. Am. Chem. Soc.*, 2004, 126, 13236.
4 (a) J.Luo,Y. Zhao,H. Xu, T. L. Kinnibrugh,D. Yang,T. V. Timofeeva, L.L. Daemen, J. Zhang, W. Bao, J. D. Thompson, and R. P. Currier, *Inorg. Chem*. 2007, 46, 9021; (b) J. B. Goodenough, Magnetism and the Chemical Bond, Wiley, NewYork, 1963.
5 (a) J.-R. Li, Q. Yu, Y. Tao, X.-H. Bu, J. Ribas, S. R. Batten, *Chem. Commun.*, 2007; 2290; (b) M. A. Nadeem, M. Bhadbhade, R. Bircher, J. A. Stride, Crystal *Growth & Design*,, 2010, 10,4060; (c) X.-Y. Wang, H.-Y. Wei, Z.-M. Wang, Z.-D. Chen, S. Gao, *Inorg. Chem*. 2005, **44**, 572 and ref cited therein.
6 (a) Lloret, F.; Munno, G.; De Julve, M.; Cano, J.; Ruiz, R.; Caneschi, A. *Angew. Chem., Int. Ed*. 1998, **37**, 135. (b) D.-F. Wong, Z.-M. Wang and S. Gao, *Chem. Soc. Rev*., 2011, **40**, 3157 and references cited therein

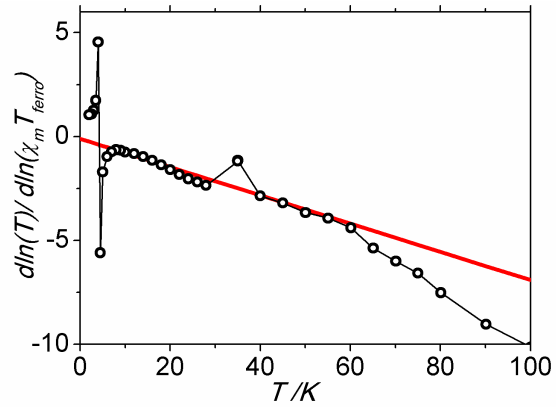

Fig. S6 Plot of the magnetic data as $dln(T)/dln(\chi_m T_{ferro})$ *vs* T for **1**. The intercepts of the red linear fitting lines with the horizontal and vertical zero axes give T_c and $1/\gamma$ respectively in which $\chi_m T_{ferro} = \chi_m T_{ferro} - C_2 \exp(\beta/T)$, C_2 and β attributed to the antiferromagnetic contribution of the fitting of the date by $\chi_m T = C_1 \exp(\alpha/T) + C_2 \exp(\beta/T)$. A direct fit of $dln(T)/dln(\chi_m T_{ferro})$ *vs* T plots the temperatures from 7 – 50 K yields $T_c = 0$ K and $g = \infty$, which is consistent with the theoretical 1D-Ising value. (ref: J. Souletie, P. Rabu and M. Drillon, Scaling Theory Applied to Low Dimensional Magnetic System in Magnetism: Molecules to Materials, vol. V ed. J. S. Miller and M. Drillon,Wiley-VCHWeinheim, Germany, 2005)

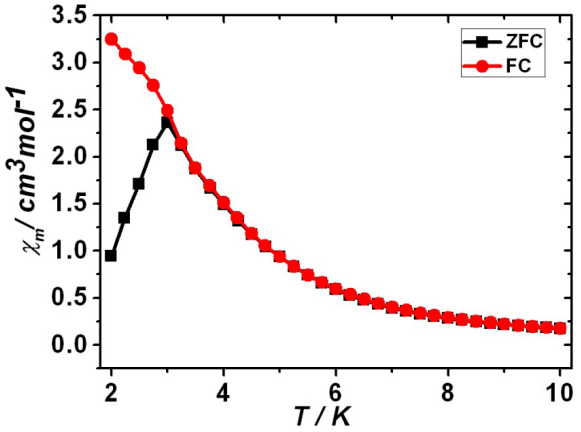

Fig. S7 Plot of ZFC and FC of **1** under 20 Oe external field.

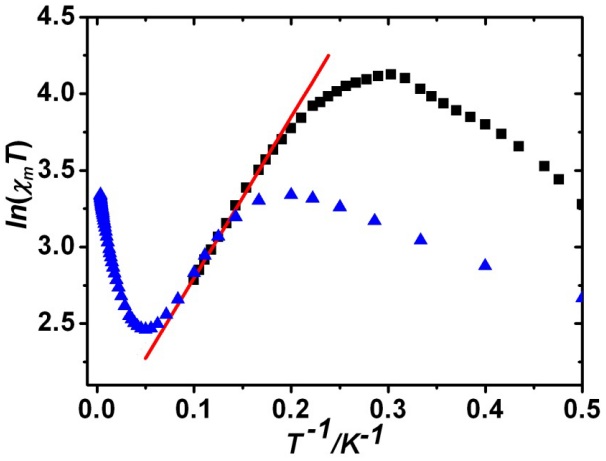

Fig. S8 Logarithm of $\chi_m T$ vs *1/T* plots (assuming eight Co^{II} ions per formula unit) of **1**. The dc susceptibility (▲) was collected at 0.2 T and the ac susceptibility (■) was obtained at a frequency of 100 Hz under oscillating field of 3 Oe. The red line is the result of fitting by $\chi_m T = C_{eff}\, exp(\Delta/k_B T)$) between 15 K and 5 K with the energy gap of Δ/k_B = 9.60 K and C_{eff} = 6.84 cm^3 mol^{-1} K.

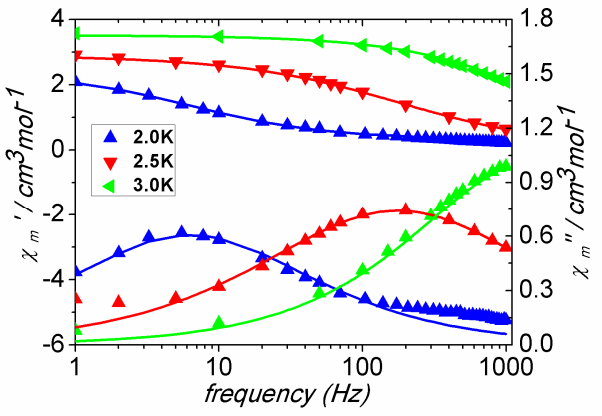

Fig. S9 Frequency dependence of *ac* susceptibilities at 2.0 K, 2.5K and 3K in zero applied dc field for **1**. The red solid line represents the least-squares fitting of the data.

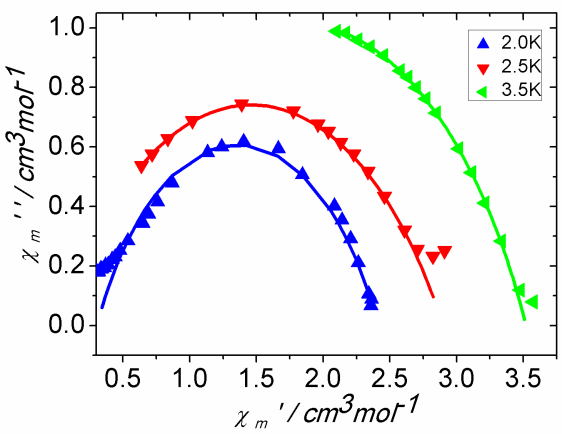

Fig. S10 Cole-Cole plot of χ_M'' vs χ_M' at 2.0 K, 2.5K and 3K in zero applied dc field for **1**. The red solid line represents the least-squares fitting of the data to a distribution of single relaxation processes.

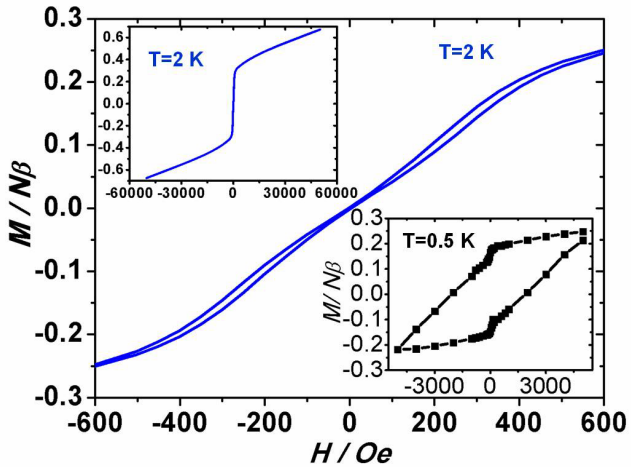

Fig. S11 Plots of hysteresis loop of **1** at 2 K and 0.5 K.